

Path Following Using Transverse Feedback Linearization: Application to a Maglev Positioning System ^{*}

Christopher Nielsen ^a, Cameron Fulford ^b, Manfredi Maggiore ^c

^a*Department of Electrical and Computer Engineering, University of Waterloo, 200 University Ave. W, Waterloo, Ontario, N2L 3G1, Canada.*

^b*Quanser Inc., 119 Spy Court, Markham, Ontario, L3R 5H6, Canada.*

^c*Electrical and Computer Engineering Department, University of Toronto, 10 King's College Road, Toronto, Ontario, M5S 3G4, Canada.*

Abstract

This article presents an approach to path following control design based on transverse feedback linearization. A “transversal” controller is designed to drive the output of the plant to the path. A “tangential” controller meets application-specific requirements on the path, such as speed regulation and internal stability. This methodology is applied to a five degree-of-freedom (5-DOF) magnetically levitated positioning system. Experimental results are provided that demonstrate the effectiveness of our control design.

Key words: path following, path following manifold, set stabilization, transverse feedback linearization, contactless positioning stage, magnetic levitation.

1 Introduction

The path following control problem (PFP) is chiefly concerned with providing a stable motion along a given path with no *a priori* time parameterization associated with the movement on the path. More specifically, the control objective is to drive the output of a control system to the path in such a way that the path is traversed in a desired direction. Usually, specific applications impose additional requirements, such as speed regulation on the path and internal stability.

PFP has some affinity to the tracking control problem, in which it is desired that the system output asymptotically matches a reference signal, but there are fundamental differences. Consider, for instance, the simple problem of making a planar kinematic point-mass vehicle follow a path on the plane. A path following controller should render the path an invariant set for the closed-loop system. In other words, if the vehicle is initialized on the path, then the vehicle should remain on it for all time. A tracking controller would make the vehicle follow a reference point moving along the path and therefore it would not guarantee invariance of the path. As a matter of fact, if the vehicle is initialized on the path, but its position does not coincide with that of the reference point, then the vehicle will leave the path and then asymptotically approach it. More generally, tracking controllers stabilize a specific system trajectory, while path following controllers should stabilize a *family* of trajectories, all those whose associated output

^{*} This paper was not presented at any IFAC meeting. This research was performed while C. Nielsen and C. Fulford were with the Dept. of Electrical and Computer Engineering, University of Toronto. Corresponding author C. Nielsen Tel. +1.519.888.4567 ext. 32241. Fax +1.519.746.3077.

Email addresses: cnielsen@uwaterloo.ca (Christopher Nielsen), fulford@control.utoronto.ca (Cameron Fulford), maggiore@control.utoronto.ca (Manfredi Maggiore).

signals lie on the desired path. We call the collection of all such trajectories the *path following manifold*. Its precise definition is given in Section 2.

The point of view taken in this paper is to convert PFP into the stabilization of the path following manifold. This guarantees, among other things, the invariance property mentioned earlier. Among various possible set stabilization techniques, we choose to use transverse feedback linearization [2], [13], which makes it possible to divide the control design into two steps: the stabilization of the path following manifold (transversal control design) and the control of the motion on the manifold (tangential control design).

We apply this methodology to the design of a path following controller for a 5-DOF magnetically levitated system at the University of Toronto Systems Control research lab. The path invariance property induced by our control method is particularly beneficial in this application, because it effectively creates virtual mechanical constraints in the system that make it act as if it were being guided by (re-configurable) mechanical guides. This distinguishes our path following controller from some others in the literature and tracking controllers.

In this paper we denote by I_m the $m \times m$ identity matrix and by $0_{m \times n}$ the $m \times n$ matrix of zeros. Let $\text{col}(x_1, \dots, x_k) := [x_1 \ \dots \ x_k]^\top$.

2 Path following methodology

We consider smooth control-affine systems with m inputs and p outputs,

$$\begin{aligned} \dot{x} &= f(x) + g(x)u, & x &\in \mathbb{R}^n \\ y &= h(x). \end{aligned} \tag{1}$$

Given a smooth embedded¹ path in the output space, $\gamma := \{y : s(y) = 0\}$, we want to design a smooth feedback that makes the output of the system (1) approach and traverse γ in a desired direction with a desired speed. Moreover, it is required that γ be output invariant for the closed-loop system. In order to give a precise definition of output invariance, let $\Gamma := \{x : s(h(x)) = 0\}$. Stabilizing the set Γ corresponds to sending the output of the plant to the desired path. However, generally Γ is not an invariant set so one should instead stabilize the maximal controlled-invariant set contained in Γ , which we denote by Γ^* . Intuitively, the set Γ^* is the collection of all those motions of the control system (1) whose associated output signals can be made to lie in γ for all time by a suitable choice of input signal.

Assumption 1 *The maximal controlled-invariant subset of $\Gamma = \{x : s(h(x)) = 0\}$, Γ^* , is a non-empty, closed embedded submanifold of the state space. Let n^* be its dimension.*

Assumption 1 is a basic feasibility requirement for the path following problem. With this assumption, Γ^* is precisely the zero dynamics manifold of the control system $\dot{x} = f(x) + g(x)u$ with output $\hat{y} = s(h(x))$.

Definition 1 *The path following manifold Γ^* of γ with respect to (1) is the maximal controlled invariant submanifold contained in $(s \circ h)^{-1}(0)$.*

Definition 2 *Let $\bar{u}(x)$ be a smooth feedback and let Γ^* be the path following manifold of γ with respect to (1). The path γ is output invariant under the closed loop vector field $\bar{f} := f + g\bar{u}$ if Γ^* is invariant under \bar{f} .*

The path following control design problem entails finding a feedback ensuring that three objectives are met.

- P1** For each initial condition in a suitable set, the corresponding solution $x(t)$ is defined for all $t \geq 0$ and $\|h(x(t))\|_\gamma \rightarrow 0$ as $t \rightarrow +\infty$, where $\|y\|_\gamma$ denotes the point-to-set distance of y to the set γ , i.e., $\|y\|_\gamma := \inf_{p \in \gamma} \|y - p\|$.
- P2** The set γ is output invariant for the closed-loop system in the sense of Definition 2.

¹ By *smooth* we mean that s is a smooth function; by *embedded* we mean that the path has no self-intersections and it is a closed subset of \mathbb{R}^p . This is equivalent to requiring that one can choose $s : \mathbb{R}^p \rightarrow \mathbb{R}^{p-1}$ so that its Jacobian has full rank $p - 1$ everywhere on γ .

P3 The motion on γ meets additional application-specific requirements such as direction and speed of traversal of the path, and boundedness of the internal dynamics.

Our approach to solving PFP is summarized below.

S1 Find the path following manifold Γ^* .

S2 Transverse feedback linearization, [13]. Find, if possible, a coordinate transformation $T : x \mapsto (\eta, \xi)$, defined in a neighbourhood U of Γ^* , and a regular feedback transformation $u = \alpha(x) + \beta(x)v$ (β non-singular on U) such that $T(\Gamma^*) = \{(\eta, \xi) : \xi = 0\}$ and, in new coordinates,

$$\begin{aligned}\dot{\eta} &= f^0(\eta, \xi) + g^\eta(\eta, \xi)v^\eta + g^\parallel(\eta, \xi)v^\parallel \\ \dot{\xi} &= A\xi + Bv^\eta\end{aligned}\tag{2}$$

with $v := \text{col}(v^\eta, v^\parallel) \in \mathbb{R}^m$ and (A, B) a controllable pair. We refer to the ξ subsystem as the *transversal subsystem*. On the other hand, the system $\dot{\eta} = f^0(\eta, 0) + g^\parallel(\eta, 0)v^\parallel$ is the *tangential subsystem*.

S3 Transversal control design. Design a transversal feedback $v^\eta(\xi)$ stabilizing the origin of the transversal subsystem.

S4 Tangential control design. Design a tangential feedback $v^\parallel(\eta, \xi)$ such that, when $\xi = 0$, the tangential subsystem meets the application-specific goals in **P3** and, moreover, the closed-loop system has no finite escape times.

The approach outlined above relies on the stabilization of the path following manifold Γ^* . Other set stabilization approaches may be used to stabilize Γ^* , but transverse feedback linearization is particularly well suited to path following because it allows one to separately address the stabilization of Γ^* (objectives **P1** and **P2**) and the control of the dynamics on Γ^* (objective **P3**). More specifically, the tangential subsystem, with state η , describes the motion on Γ^* , that is when the plant output lies in γ . The tangential controller is designed to prevent finite escape times from occurring and to meet goal **P3**. The transversal subsystem, with state ξ , describes the motion off the set Γ^* . Due to the absence of finite escape times, the transversal controller stabilizes $T(\Gamma^*)$. If the trajectories of the closed-loop system are bounded², then the stabilization of $T(\Gamma^*)$ implies that of Γ^* , and therefore the transversal controller meets goal **P1**. It also meets goal **P2** because the origin of the ξ subsystem is an equilibrium of the closed-loop system, and thus Γ^* is an invariant set of the closed-loop system.

Notice that transverse feedback linearization amounts to partial feedback linearization with the additional requirement that the linear subsystem be representative of the dynamics transversal to the target set Γ^* . This additional requirement may result in nonlinear dynamics for the tangential subsystem even when (1) is exactly feedback linearizable.

The computation, in step **S1**, of Γ^* can be performed using the zero dynamics algorithm described in [8], provided some mild regularity conditions hold. In general, however, the algorithm only provides a characterization of Γ^* in the neighbourhood of a point. One may, if needed, apply the algorithm in a neighbourhood of various points to piece together Γ^* . We now discuss the existence and derivation of the coordinate and feedback transformations that are required in step **S2** to get the normal form (2) with the property that $T(\Gamma^*) = \{(\eta, \xi) : \xi = 0\}$. The transformations in question are guaranteed to exist locally around any point of Γ^* (see [13]) if and only if there exist functions $\alpha_1(x), \dots, \alpha_l(x)$, $1 \leq l \leq m$, with the following properties.

- (a) $\Gamma^* \subset \{x : \alpha_1(x) = \dots = \alpha_l(x) = 0\}$.
- (b) The “virtual” output $\alpha(x) = \text{col}(\alpha_1(x), \dots, \alpha_l(x))$ yields a uniform vector relative degree $\{k_1, \dots, k_l\}$ on Γ^* and the indices k_i are such that $k_1 + \dots + k_l = n - n^*$.

A good first guess for the required virtual output is the function $s(h(x))$, or a function defined using some of the components of $s(h(x))$, because it already satisfies property (a) above. If this guess doesn’t work, then Theorem 3.2 in [13] gives necessary and sufficient checkable conditions for the existence of the required functions. More comments on the derivation of $\alpha_1, \dots, \alpha_l(x)$ are found in [13]. Now suppose that $\alpha_1(x), \dots, \alpha_l(x)$ have been found that satisfy properties (a) and (b). We show how they are used to derive the normal form (2). Let $D(x)$ be the decoupling matrix associated to the output $\alpha(x)$, i.e., the $l \times m$ matrix with components $D_{ij}(x) = L_{g_j} L_f^{k_i - 1} \alpha_i(x)$ which,

² It may happen in some applications that the trajectories of the closed-loop system aren’t bounded because the path itself is unbounded. In this case, in order to be able to state that the stabilization of $T(\Gamma^*)$ implies that of Γ^* , it is necessary that there exist a class- \mathcal{K} function α such that $\xi(x) \geq \alpha(\|x\|_{\Gamma^*})$.

by property (b), has rank l on Γ^* and therefore also on a neighbourhood \mathcal{N} of Γ^* . Let $\beta(x) = [M(x) \ N(x)]$, where $M(x) := D^\top(x)(D(x)D^\top(x))^{-1}$ is the $m \times l$ right-inverse of $D(x)$, and $N(x)$ is a $m \times (m-l)$ smooth matrix-valued function whose columns span³ the kernel of $D(x)$. Notice that $\beta(x)$ just defined is non-singular. Let $\alpha(x) = -\beta(x) \text{col}(L_f^{k_1} \alpha_1, \dots, L_f^{k_l} \alpha_l, 0_{m-l \times 1})$. Consider the feedback transformation $u = \alpha(x) + \beta(x)v$, where $v = \text{col}(v^\perp, v^\parallel)$, with $v^\perp \in \mathbb{R}^l$ and $v^\parallel \in \mathbb{R}^{m-l}$. This feedback transformation and property (b) give

$$\begin{bmatrix} d^{k_1} \alpha_1 / dt \\ \vdots \\ d^{k_l} \alpha_l / dt \end{bmatrix} = \begin{bmatrix} L_f^{k_1} \alpha_1 \\ \vdots \\ L_f^{k_l} \alpha_l \end{bmatrix} + D(x)(\alpha(x) + \beta(x)v) = v^\perp.$$

Defining the map $x \mapsto \xi$ as

$$\xi := \text{col}(\alpha_1, \dots, L_f^{k_1-1} \alpha_1, \dots, \alpha_l, \dots, L_f^{k_l-1} \alpha_l)(x),$$

the above implies that $\dot{\xi} = A\xi + Bv^\perp$, where (A, B) is in Brunowský normal form with controllability indices $\{k_1, \dots, k_l\}$. Next, following the ideas in the proof of Proposition 11.5.1 in [9], one finds that there exists a map $\eta = \varphi(x)$ mapping a neighbourhood of Γ^* onto Γ^* such that the transformation $T : x \mapsto (\eta, \xi)$ is a diffeomorphism mapping a neighbourhood of Γ^* onto a neighbourhood of $\Gamma^* \times \mathbb{R}^{n-n^*}$. In transformed coordinates, the dynamics have precisely the form (2). It can also be shown, using a straightforward argument found in the proof of Theorem 4.1 in [12], that $T(\Gamma^*) = \{(\eta, \xi) : \xi = 0\}$. This concludes the derivation of the normal form in step **S2**.

3 Comparison of path following approaches in the literature

Early investigations of the path following problem in [16], [17] focus on specific applications and rely on coordinate transformations decomposing the system dynamics into tangential and transversal components. These approaches are therefore similar to ours.

Another approach is to parameterize the path, use the parameterization as a reference trajectory, and treat the velocity of the reference point as an extra control input. This approach, and variations on its theme, is popular and is the subject of a considerable amount of work, see [1], [4], [7], [11] among others. An interesting feature in these papers is that they divide the control design into two subproblems; the geometric task achieves convergence to the path, while the dynamic task assigns a speed profile on the path. In our framework, the transversal control design addresses the geometric task, while the tangential control design addresses the dynamic task. On the other hand, relying on a parameterization of the path, the above mentioned approaches share the drawback of all tracking controllers mentioned in the introduction in that they fail to make the path output invariant.

Research has also been devoted to the study of the *exact* (or *perfect*) path following problem for specific applications. The exact path following problem entails finding a trajectory of the control system and an open-loop control such that the corresponding output signal traces the required path in its entirety. We refer the reader to [3] and [14] for two representative approaches to this problem. The relationship to our approach is that any trajectory solving the perfect path following problem must *necessarily* lie on the path following manifold Γ^* . In general, there might be more than one trajectory solving the exact path following problem and therefore, generally, Γ^* has dimension greater than one. The idea of stabilizing the whole Γ^* , rather than just one trajectory on Γ^* allows one to change the motion along the path, by means of the tangential control design in step **S4**, without having to repeat the control design process. There are times when the motion on the path is completely determined by the requirement of making the trajectory manifold invariant. In this case, all the control effort goes towards the stabilization of Γ^* [18]; there are no “tangential” controls. This may be the case, for example, in trying to stabilize a Jordan curve in the configuration space of an underactuated controlled Euler-Lagrange system [18].

³ Since $D(x)$ has constant rank around Γ^* , for each point p in Γ^* there exists a smooth matrix-valued function $N(x)$, defined in a neighbourhood of p , spanning the kernel of D . This isn't enough, as we want to define $N(x)$ over a neighbourhood of Γ^* on which D has full rank (possibly the whole \mathcal{N}). If \mathcal{N} is a contractible set (i.e., if it can be continuously deformed to a point), then in fact one can find $N(x)$ defined over the whole \mathcal{N} .

4 Experimental apparatus and model

4.1 Hardware setup

The 5-DOF maglev positioning system was developed in collaboration with Quanser and is the evolution of two previous setups, a 2-DOF and a 3-DOF, described in [15]. The setup used in this research, described in greater detail in [6], consists of four symmetrically placed iron-cored permanent magnet linear synchronous motors, or PMLSMs. Each PMLSM consists of a stator and a mover. The stators are housed in a heavy stationary frame and each mover is positioned beneath its corresponding stator and affixed to an aluminium platen. Each stator exerts two orthogonal forces on the mover: a horizontal translational force and a vertical normal force. The aluminium platen is positioned below a stationary frame and rests on sets of linear guides that allow the platen to move along two horizontal axes, one vertical axis, as well as rotate about the two horizontal axes (pitch and roll). The linear guides do not provide any actuation force to the platen other than friction (a disturbance) and are currently required to maintain proper alignment of the platen and, most importantly, facilitate the placement of sensors used to measure displacements and rotations of the platen. The system has a horizontal displacement range of ± 50 mm along the X-axis and Z-axis, a vertical range of approximately 13 mm, and rotations about the X-axis and Z-axis of approximately ± 3 mrad and ± 14 mrad, respectively. Let $\mathcal{T} = [0.018, 0.031] \times [-0.05, 0.05] \times [-0.05, 0.05]$ and $\mathcal{R} = [-0.003, 0.003] \times [-0.014, 0.014]$ denote the allowable operating range of the translational and rotational subsystems measured in meters and radians, respectively.

4.2 Mathematical model

The mathematical model of the forces produced by an iron-cored permanent magnet linear synchronous motor (PMLSM) was reported in [10]. Using this model it is a simple matter to derive the dynamics describing the translations and two rotations of the platen. The detailed derivation is found in [5], [6]. For the sake of clarity and conciseness, we will not present the cumbersome expressions of the forces and the derivation of the mathematical model. We will rather focus on presenting its basic structure.

We denote by x_1 , x_3 , and x_5 the Y, X, and Z-axes displacements of the centre of mass of the platen, respectively, and by x_2 , x_4 , and x_6 their velocities. Note that $(x_1, x_3, x_5) \in \mathcal{T}$. Furthermore, we let x_7 and x_9 denote the rotation angles of the platen about the X and Z-axes, respectively, and by x_8 and x_{10} the corresponding angular velocities. We have that $(x_7, x_9) \in \mathcal{R}$. Our convention is that when $x_1 = 0.025$ and $x_3 = x_5 = x_7 = x_9 = 0$ the platen is placed in the centre of its displacement range and it is levelled with the ground.

The physical inputs to the system are the applied three-phase currents to each of the PMLSMs. It is customary to represent three-phase currents of motor k , $k \in \{1, 2, 3, 4\}$, using their direct and quadrature components, which we denote by i_{d_k} and i_{q_k} . Having eight control inputs, the system is overactuated. We now briefly describe how to eliminate the overactuation. Set $u_x := i_{q_2} = i_{q_4}$, $u_z := i_{q_1} = i_{q_3}$, to make sure that when the platen is levelled with the ground the horizontal forces produced by motor pairs (2,4) and (1,3) are the same. We further set $u_y := i_{d_1} + i_{d_3} = i_{d_2} + i_{d_4}$, $u_\phi := i_{d_1} - i_{d_3}$, $u_\theta := i_{d_2} - i_{d_4}$. The definition of u_y guarantees that when the platen is levelled with the ground motor pairs (1,3) and (2,4) produce the same lift force. On the other hand, roughly speaking, u_ϕ and u_θ are mostly responsible for actuating the rotations around the Z and X-axes, respectively. We thus have five control inputs $(u_x, u_z, u_y, u_\phi, u_\theta)$ that actuate 5-DOFs.

With this definition, a simplified⁴ mathematical model of the system has the form (3). The state space of the system is $\mathcal{X} := \mathbb{R}^6 \times \mathbb{S}^1 \times \mathbb{R} \times \mathbb{S}^1 \times \mathbb{R}$, where \mathbb{S}^1 denotes the unit circle. The system output is given by the three displacements, $h(x) := \text{col}(x_1, x_3, x_5)$. For the remainder of this paper we will call $(x_1, x_2, x_3, x_4, x_5, x_6)$ the *translational subsystem*

⁴ In reality, the mathematical model of the plant is not affine in the control inputs u_y, u_ϕ , and u_θ , due to the presence of quadratic expressions involving these currents. However, the analysis in [5] shows that the control-affine approximation of the model describes the dynamics of the control system sufficiently well for control purposes.

and (x_7, x_8, x_9, x_{10}) the *rotational subsystem*.

$$\begin{aligned}
\dot{x}_1 &= x_2 \\
\dot{x}_2 &= a_1(x_1, x_7, x_9, u_x, u_z) + a_2(x_1, x_7, x_9)u_y \\
&\quad + a_3(x_1, x_7)u_\phi + a_4(x_1, x_9)u_\theta \\
\dot{x}_3 &= x_4 \\
\dot{x}_4 &= p(x_1, x_9)u_x \\
\dot{x}_5 &= x_6 \\
\dot{x}_6 &= q(x_1, x_7)u_z \\
\dot{x}_7 &= x_8 \\
\dot{x}_8 &= b_1(x_1, x_7, u_z) + b_2(x_1, x_7)u_y + b_3(x_1, x_7)u_\phi \\
\dot{x}_9 &= x_{10} \\
\dot{x}_{10} &= c_1(x_1, x_9, u_x) + c_2(x_1, x_9)u_y + c_3(x_1, x_9)u_\theta.
\end{aligned} \tag{3}$$

All functions in the above model are smooth. Their salient properties are listed below

- $b_1(x_1, 0, u_z) \equiv b_2(x_1, 0) \equiv c_1(x_1, 0, u_x) \equiv c_3(x_1, 0) \equiv 0$.
- The functions $p(x_1, x_9), q(x_1, x_7), b_3(x_1, x_7), c_3(x_1, x_9)$ do not vanish on $\mathcal{T} \times \mathcal{R}$.
- Letting

$$K(x) := \begin{bmatrix} a_2(x_1, x_7, x_9) & a_3(x_1, x_7) & a_4(x_1, x_9) \\ b_2(x_1, x_7) & b_3(x_1, x_7) & 0 \\ c_2(x_1, x_9) & 0 & c_3(x_1, x_9) \end{bmatrix},$$

it can be shown numerically that the matrix $K(x)$ is nonsingular on $\mathcal{T} \times \mathcal{R}$.

These properties readily imply that the model (3) is controllable at any equilibrium configuration in $\mathcal{T} \times \mathcal{R}$.

5 Path following control design

We want to solve the path following control problem, formulated in Section 2, with path γ given by a closed Jordan curve in the output space. To concretely illustrate our design, we pick an ellipse not levelled with the ground,

$$\gamma := \{(y_1, y_2, y_3) \in \mathbb{R}^3 : s_1(y) = s_2(y) = 0\}, \tag{4}$$

$s_1(y) := y_2^2 + y_3^2 - 0.03^2$, $s_2(y) := -18y_1 + 3y_2 + 0.45$, but our procedure can be applied to any other embedded path that is expressible as the zero level set of a function. The ellipse (4) covers most of the operating range \mathcal{T} for the displacements. The controller must meet objectives **P1-P3** in Section 2 with **P3** specialized to this application as follows,

- P3** On the path γ , $(x_1(t), x_3(t), x_5(t))$ tracks a desired speed profile. Moreover, the rotational dynamics are regulated to zero, i.e., $(x_7(t), x_8(t), x_9(t), x_{10}(t)) \rightarrow 0$ as $t \rightarrow \infty$.

5.1 Preliminary feedback transformation

The first step in controller design is to observe that the plant (3) is feedback linearizable. The feedback transformation

$$\begin{bmatrix} u_x \\ u_z \end{bmatrix} = \begin{bmatrix} u_2/p(x_1, x_9) \\ u_3/q(x_1, x_7) \end{bmatrix} \\ \begin{bmatrix} u_y \\ u_\phi \\ u_\theta \end{bmatrix} = K(x)^{-1} \begin{bmatrix} u_1 - a_1(x_1, x_7, x_9, u_x, u_z) \\ u_4 - b_1(x_1, x_7, x_9, u_z) \\ u_5 - c_1(x_1, x_9, u_x) \end{bmatrix}, \quad (5)$$

gives five decoupled double-integrators with input $u := (u_1, \dots, u_5)$ and dynamics $\dot{x} = \hat{A}x + \hat{B}u$ where \hat{A} and \hat{B} are in Brunowský normal form. We next apply the procedure presented in Section 2 to system $\dot{x} = \hat{A}x + \hat{B}u$ with path (4).

5.2 Step 1: Finding the path following manifold

The path following manifold Γ^* is the maximal control invariant subset of $\Gamma = \{x : s_1(h(x)) = 0, s_2(h(x)) = 0\}$, with $s_1(h(x)) = x_3^2 + x_5^2 - 0.03^2$ and $s_2(h(x)) = -18x_1 + 3x_3 + 0.45$. In this case, the task of finding Γ^* is straightforward because the virtual output $\hat{y} := \text{col}(s_1(h(x)), s_2(h(x)))$ yields a well-defined vector relative degree of $\{2, 2\}$ on $\mathcal{X}/\{x : x_3 = x_5 = 0\}$ since the decoupling matrix

$$D(x) = \begin{bmatrix} 0 & 2x_3 & 2x_5 & 0 & 0 \\ -18 & 3 & 0 & 0 & 0 \end{bmatrix}$$

has full rank on $\mathcal{X}/\{x : x_3 = x_5 = 0\}$. Therefore the path following manifold has dimension $n^* = 6$ and is given by

$$\Gamma^* = \left\{ x \in \mathcal{X} : \begin{aligned} x_3^2 + x_5^2 - 0.03^2 &= -18x_1 + 3x_3 + 0.45 = \\ 2x_3x_4 + 2x_5x_6 &= -18x_2 + 3x_4 = 0 \end{aligned} \right\}. \quad (6)$$

5.3 Step 2: Transverse feedback linearization

Since the virtual output $\hat{y} = \text{col}(s_1(h(x)), s_2(h(x)))$ yields a well-defined vector relative degree, the derivation of the normal form (2) amounts to standard input-output feedback linearization. Following the procedure for deriving the normal form outlined in Section 2, let $\beta(x) = [M(x) \ N(x)]$, where $M(x) = D^\top(x)(D(x)D^\top(x))^{-1}$ is the right-inverse of $D(x)$ and the columns of

$$N(x) = \left[\begin{array}{c|c} x_5 & \\ \hline 6x_5 & 0_{3 \times 2} \\ -6x_3 & \\ \hline 0_{2 \times 1} & I_2 \end{array} \right]$$

span the kernel of $D(x)$, and define the feedback transformation

$$\begin{aligned} u &= -\beta(x) \text{col}(2(x_4^2 + x_6^2), 0, 0, 0, 0) + \beta(x)v, \\ v &= (v_1^\uparrow, v_2^\uparrow, \hat{v}_1^\parallel, v_2^\parallel, v_3^\parallel). \end{aligned} \quad (7)$$

Notice that this feedback transformation is regular on $\mathcal{X}/\{x : x_3 = x_5 = 0\}$. Next, the state of the transversal subsystem is defined as

$$\xi := \begin{bmatrix} \hat{y}_1 \\ \dot{\hat{y}}_1 \\ \hat{y}_2 \\ \dot{\hat{y}}_2 \end{bmatrix} = \begin{bmatrix} x_3^2 + x_5^2 - 0.03^2 \\ 2x_3x_4 + 2x_5x_6 \\ -18x_1 + 3x_3 + 0.45 \\ -18x_2 + 3x_4 \end{bmatrix}. \quad (8)$$

We complete the coordinate transformation by means of the map $x \mapsto \eta$ defined below,

$$\begin{aligned} \eta_1 &= \arg(x_3 + ix_5) \\ \eta_2 &= (x_3x_6 - x_4x_5)/(x_3^2 + x_5^2) \\ \eta_3 &= x_7 \\ \eta_4 &= x_8 \\ \eta_5 &= x_9 \\ \eta_6 &= x_{10}. \end{aligned} \quad (9)$$

The state η_1 is the angle formed by the projection of the centre of mass of the platen onto the $X - Z$ plane and the X -axis, and η_2 represents the corresponding angular velocity. The transformation $T : x \mapsto (\eta, \xi)$ defined by (8) and (9) is a diffeomorphism of $\mathcal{X}/\{x : x_3 = x_5 = 0\}$ onto its image and it yields the desired normal form,

$$\begin{aligned} \dot{\eta}_1 &= \eta_2 \\ \dot{\eta}_2 &= \phi(x, v_1^{\hat{\cdot}}, v_2^{\hat{\cdot}}) - 6\hat{v}_1^{\parallel} \\ \dot{\eta}_3 &= \eta_4 \\ \dot{\eta}_4 &= v_2^{\parallel} \\ \dot{\eta}_5 &= \eta_6 \\ \dot{\eta}_6 &= v_3^{\parallel} \\ \dot{\xi} &= A\xi + Bv^{\hat{\cdot}}. \end{aligned}$$

where $\phi(x, v_1^{\hat{\cdot}}, v_2^{\hat{\cdot}})$ is a smooth function defined on $\mathcal{X}/\{x : x_3 = x_5 = 0\}$. Interestingly, the system above is feedback equivalent to a linear time-invariant system. For, by letting

$$\hat{v}_1^{\parallel} = 1/6(\phi(x, v_1^{\hat{\cdot}}, v_2^{\hat{\cdot}}) - v_1^{\parallel}), \quad (10)$$

we obtain the linear time-invariant system

$$\begin{aligned} \dot{\eta} &= A^*\eta + B^*v^{\parallel} \\ \dot{\xi} &= A\xi + Bv^{\hat{\cdot}}, \end{aligned} \quad (11)$$

where (A^*, B^*) and (A, B) are in Brunowsky normal form and represent, respectively, three decoupled double-integrators and two decoupled double-integrators. Remarkably, while in the general normal form (2) the η -subsystem is coupled to the transversal subsystem, in (11) the two subsystems in question are decoupled.

5.4 Step 3: Transversal control design

We stabilize the origin of the transversal subsystem in (11), therefore meeting design goals **P1** and **P2**, by means of two parallel PID compensators,

$$\begin{aligned} v_1^{\hat{\cdot}}(\xi) &= -K_{11}\xi_1 - K_{12}\xi_2 - K_{13} \int_0^t \xi_1(\tau)d\tau \\ v_2^{\hat{\cdot}}(\xi) &= -K_{21}\xi_3 - K_{22}\xi_4 - K_{23} \int_0^t \xi_3(\tau)d\tau. \end{aligned}$$

Since $v_1^{\hat{\cdot}}(0) = v_2^{\hat{\cdot}}(0) = 0$, $\xi = 0$ is an equilibrium of the closed-loop transversal subsystem in (11), and thus Γ^* is an invariant set for the closed-loop system. In other words, the controller above meets goal **P2**. The positive gains K_{ij} are selected using LQR design with manual tuning of the weight matrices.

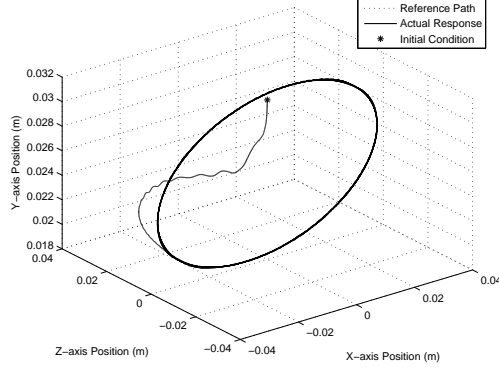


Fig. 1. Position response of the path following controller

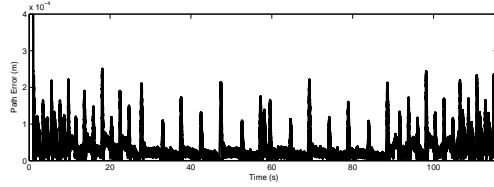


Fig. 2. Path error measured for the path following controller at various velocities

5.5 Step 4: Tangential control design

We now design a tangential controller for the η -subsystem in (11) that meets objective **P3**. Recalling the definition of η in (9), making sure that, on γ , the centre of mass of the platen (x_1, x_2, x_3) tracks a desired speed profile is equivalent to making sure that the angular velocity η_2 approaches a desired reference profile $\eta_2^{\text{ref}}(t)$, which can be achieved by means of a simple proportional feedback with feedforward action. Furthermore, regulating the rotational dynamics corresponds to stabilizing the origin of the subsystem with states $(\eta_3, \eta_4, \eta_5, \eta_6)$, which can be achieved by means of two PID compensators. In the light of the above, the tangential controller

$$\begin{aligned} v_1^{\parallel}(\eta) &= \dot{\eta}_2^{\text{ref}}(t) - K_3(\eta_2 - \eta_2^{\text{ref}}(t)) \\ v_2^{\parallel}(\eta) &= -K_{41}\eta_3 - K_{42}\eta_4 - K_{43} \int_0^t \eta_3(\tau) d\tau \\ v_3^{\parallel}(\eta) &= -K_{51}\eta_5 - K_{52}\eta_6 - K_{53} \int_0^t \eta_5(\tau) d\tau \end{aligned}$$

meets design goal **P3**. The positive gains in the above controller are chosen using LQR design with manual tuning of the weight matrices.

6 Experimental Results

We define the instantaneous “path error”, denoted $e(t)$, as the minimum Euclidean distance of the center of mass of the platen to the path at time t , $e(t) := \|(x_1(t), x_3(t), x_5(t))\|_{\gamma}$. The average path error over a finite time interval $[0, T]$ is $\bar{e}(T) := \frac{1}{T} \int_0^T e(\tau) d\tau$. The average path error is the performance metric throughout the tuning process.

We ran a test consisting of a series of constant angular velocity commands $\{\pi/2, \pi/4, \pi/8, -\pi/8, -\pi/4, -\pi/2\}$ rad/s. For each velocity, the platen was moved through two circuits around the path before switching to the next velocity command. The initial average path error for this test was over $300\mu\text{m}$, and after tuning the average path error was reduced to approximately $41\mu\text{m}$. Figure 1 shows the position response of the system after tuning in XYZ space. Figure 2 shows the measured path error during the test. The performance is clearly satisfactory.

Next we ran longer trials at constant velocities ranging from $\pi/8$ rad/s to 2π rad/s and recorded the average path error with $T = 60$ seconds for each velocity. Figure 3 summarizes the results from this test. We observe a large increase in average path error as the speed increases.

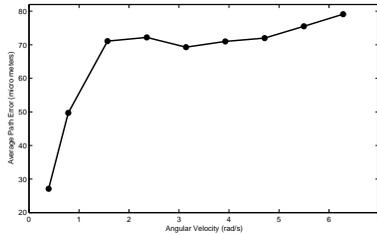


Fig. 3. Average path error measured over 60 seconds for various angular velocities

There was a significant friction effect at points where the platen’s motion along an axis stops and changes direction. We call these *turn-around points*. We say that this is predominantly a friction effect for two reasons: 1) the effect is symmetrical and depends on the direction of travel, and 2) the effect is less predominant at larger velocities when the platen has more persistency of motion. Figure 4 illustrates the effect (before controller tuning) at velocities $\pi/8$ and $-\pi/8$.

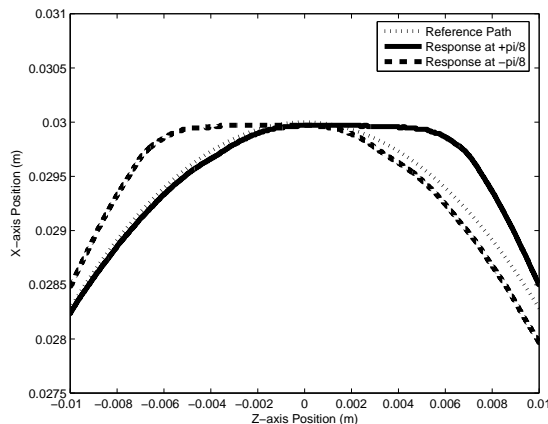


Fig. 4. Effect of friction at a turn-around point for small velocities

We also observed a slight coupling between the η and ξ dynamics, that theoretically (see (11)) are decoupled. This coupling manifests itself by an increase in the average path error at large angular velocities η_2 . This is evidenced in Figure 3, which shows the measured average path errors for various angular velocities. Through tuning of control parameters, we were able to reduce the average path error from over $300 \mu\text{m}$ to approximately $41 \mu\text{m}$. We conjecture that the slight coupling between η and ξ subsystem is due to the simplification, in model (3), in eliminating quadratic terms involving in the motor currents.

Acknowledgements

C. Fulford was partially supported by the National Science and Engineering Research Council of Canada (NSERC) and the Canadian Fund for Innovation (CFI). C. Nielsen and M. Maggiore were supported by NSERC. The authors wish to thank Jacob Apkarian at Quanser for his help and support.

References

- [1] A.P. Aguiar and J.P. Hespanha. Trajectory-tracking and path-following of underactuated autonomous vehicles with parametric uncertainty. *IEEE Trans. on Automatic Control*, 52(8):1362–1378, 2007.

- [2] A. Banaszuk and J. Hauser. Feedback linearization of transverse dynamics for periodic orbits. *Systems and Control Letters*, 26(2):95–105, Sept. 1995.
- [3] L. Consolini and M. Tosques. On the VTOL exact tracking with bounded internal dynamics via a Poincaré map approach. *IEEE Trans. on Automatic Control*, 52(9):1757–1762, 2007.
- [4] D.B. Dačić, D. Nešić, and P. Kokotović. Path-following for nonlinear systems with unstable zero dynamics. *IEEE Trans. on Automatic Control*, 52(3):481–487, 2007.
- [5] C. Fulford. Control of a high-precision positioning system using magnetic levitation. Master’s thesis, University of Toronto, 2007.
- [6] C. Fulford, M. Maggiore, and J. Apkarian. Control of a 5DOF magnetically levitated positioning stage. *IEEE Transactions on Control Systems Technology*, 17(4):844–852, 2009.
- [7] I.A.F. Ihle, M. Arcak, and T.I. Fossen. Passivity-based designs for synchronized path-following. *Automatica*, 43(9):1508–1518, 2007.
- [8] A. Isidori. *Nonlinear Control Systems*. Springer, New York, 3rd edition, 1995.
- [9] A. Isidori. *Nonlinear Control Systems II*. Springer-Verlag, London, 1999.
- [10] M. Maggiore and R. Becerril. Modeling and control design for a magnetic levitation system. *Int. J. Control*, 77(10):964–977, 2004.
- [11] D.E. Miller and R.H. Middleton. On limitations to the achievable path following performance for linear multivariable plants. *IEEE Transactions on Automatic Control*, 53(11):2586 – 2601, 2008.
- [12] C. Nielsen and M. Maggiore. Output stabilization and maneuver regulation: A geometric approach. *Systems Control Letters*, 55:418–427, 2006.
- [13] C. Nielsen and M. Maggiore. On local transverse feedback linearization. *SIAM Journal on Control and Optimization*, 47(5):2227–2250, 2008.
- [14] G. Notarstefano, J. Hauser, and R. Frezza. Trajectory manifold exploration for the PVTOL aircraft. In *Proc. of the IEEE Conference on Decision and Control and European Control Conference*, pages 5848–5853, Seville, Spain, December 2005.
- [15] B. Owen, M. Maggiore, and J. Apkarian. A high-precision, magnetically levitated positioning stage. *IEEE Control Systems Magazine*, 26(03):82–95, June 2006.
- [16] O. Sjørdalen and C.C. de Wit. Path-following and stabilization of a mobile robot. In *Proc. of the IFAC symposium on Nonlinear Control Systems Design*, pages 477–484, 1992.
- [17] C. Samson. Control of chained systems: Applications to path following. *IEEE Trans. on Automatic Control*, 40(1):64–77, 1995.
- [18] A. Shiriaev, J.W. Perram, and C. Canudas de Wit. Constructive tool for orbital stabilization of underactuated nonlinear systems: Virtual constraints approach. *IEEE Transactions on Automatic Control*, 50(8):1164–1176, August 2005.